



Published by Avanti Publishers  
**International Journal of Architectural  
Engineering Technology**

ISSN (online): 2409-9821



## Determining Payback Period and Comparing Two Small-Scale Vertical Axis Wind Turbines Installed at the Top of Residential Buildings

Yousif Abed Saleh Saleh <sup>1</sup>, Miguel Chen Austin <sup>2</sup>, Cristina Carpino <sup>3</sup> and Cihan Turhan <sup>4,\*</sup>

<sup>1</sup>Department of Mechanical Engineering, Atılım University, Ankara 06830, Turkey

<sup>2</sup>Faculty of Mechanical Engineering, Universidad Tecnológica de Panamá, Panama City 0819-07289, Panama

<sup>3</sup>Department of Mechanical, Energy and Management Engineering, University of Calabria, Via Pietro Bucci 46C, 87036 Rende, Italy

<sup>4</sup>Department of Energy System Engineering, Atılım University, Ankara 06830, Turkey

### ARTICLE INFO

Article Type: Research Article

Academic Editor: Yidong Xu <sup>id</sup>

Keywords:

Pay-Back period

Ice-Wind turbine

Energy consumption

Residential buildings

Savonius wind turbine

Timeline:

Received: June 24, 2024

Accepted: July 29, 2024

Published: August 22, 2024

Citation: Saleh YAS, Austin MC, Carpino C, Turhan C. Determining payback period and comparing two small-scale vertical axis wind turbines installed at the top of residential buildings. Int J Archit Eng Technol. 2024; 11: 1-16.

DOI: <https://doi.org/10.15377/2409-9821.2024.11.1>

### ABSTRACT

In recent years, residential buildings have seen a notable increase in energy consumption. To address this, it is crucial for researchers to invest in renewable energy technologies, aiming to develop highly sustainable and nearly-zero energy buildings. Many countries are started to commit to this goal, seeking to phase out fossil fuels due to their harmful environmental effects. Wind energy stands out as a promising renewable resource, especially in areas with strong wind patterns. This study focuses on a case in Karaburun, Izmir province, Türkiye, where annual wind speeds range from 6 to 8 m/s and evaluates the performance of two types of small-scale Vertical Axis Wind Turbines (VAWTs) in reducing energy consumption in a three-story residential building, along with associated costs. Utilizing advanced simulation tools like ANSYS Fluent and DesignBuilder Software, the study examines Ice-Wind VAWTs and Savonius VAWTs. The findings reveal that installing 15 Ice-Wind VAWTs on the building's roof can reduce energy consumption by approximately 22.5%, with each turbine costing about \$2000 and a payback period of around 14.57 years. Conversely, using 15 Savonius VAWTs can reduce energy consumption by 36%, with each turbine costing about \$2300 and a payback period of around 8.93 years. These results indicate that the Savonius turbine offers a faster return on investment compared to the Ice-Wind turbine under the specified conditions. Overall, this study highlights the significant benefits and cost implications of integrating renewable energy solutions like VAWTs into residential buildings.

\*Corresponding Author

Email: [cihan.turhan@atilim.edu.tr](mailto:cihan.turhan@atilim.edu.tr)

Tel: +(90) 543 7975845

# 1. Introduction

Global warming has intensified as a result of the substantial rise in energy consumption, spurred by population growth, economic development, and extensive land use. Research indicates that buildings account for one-third of global energy consumption, with a large share of this energy still sourced from non-renewable resources such as gas and fossil fuels [1, 2]. Consequently, it is essential for researchers to implement renewable energy solutions and adopt diverse energy-efficient design strategies to reduce energy usage in residential buildings [3]. Türkiye has become the 16th largest energy consumer, experiencing an average annual increase in electricity consumption of 5% over the past 20 years [4].

In 2023, wind and solar energy accounted for about 20% of Türkiye's total energy production, yet there is still significant untapped potential in these resources [5, 6]. According to a report by the International Renewable Energy Agency (IRENA) for the G20, achieving temporal and geographical flexibility in the power system necessitates a variety of solutions, tailored to the system's characteristics and the availability of wind and solar energy [7].

Modern research has focused on the need to improve energy efficiency relating to building construction by using new generation technologies and materials. For instance, the incorporation of smart building systems, like intelligent energy management systems and IoT connected devices can bring down the energy consumption greatly [8-10]. Further, the use of high performing insulation materials and energy efficient windows is very important in reducing energy consumption and effective thermal comfort [11-13]. The implementation of sustainable energy solutions including photovoltaic and wind turbine have also been proven to reduce significantly the carbon footprints in dwelling and commercial buildings [14-16]. Also, policy management structures and monetary motivators have been recognized to play a major role in encouraging the use of these technologies towards realizing sustainability objectives [17-19]. Moreover, energy harvesting storage and technologies for transparency in building constructions to address the effective balance of energy needs in buildings with that of natural lighting. Comprehensive policies in the developing countries are also providing a boost to the establishment of renewable energy systems in the building sector [20-22].

This study focuses on the novel application of Ice-Wind and Savonius VAWTs in urban residential settings, providing a comparative analysis of energy efficiency and economic feasibility, including payback periods. This research fills a gap by exploring these turbines' practical integration into residential buildings, a less-explored area in the literature.

Fig. (1) shows how energy consumption is distributed across various sectors. The transport sector is the largest consumer, making up 29.2% of total energy use, and includes road, rail, air, and maritime transportation. The residential sector comes next, with households consuming 27.9% of the energy for heating, cooling, lighting, and appliances. The industrial sector, which encompasses manufacturing, construction, and mining, accounts for 25.6% of total energy consumption. The services sector, which includes commercial buildings and services, uses 13.8% of the energy. Finally, the "Other" category represents 3.6% of energy consumption. This distribution underscores the significant energy demands of the transport and residential sectors, highlighting the need for focused energy efficiency measures in these areas to achieve overall energy saving.

Numerous recent studies have been conducted focusing on wind energy, exploring its potential, efficiency, and implementation strategies. For instance, Calautit and Johnstone [23] examined small-scale wind energy technologies for building integration, focusing on wind turbines and vibration systems. Despite challenges like turbulence and structural compatibility, these technologies can generate power from milliwatts to kilowatts, suitable for low-powered sensors. Significant research gaps remain, especially in practical applications and comprehensive analyses. Xu *et al.* [24] used high-resolution numerical simulations to study vertical axis wind turbine (VAWT) arrays between buildings. They found that VAWT arrays increased power coefficients by 30% due to the blockage effect and performed best in contraction acceleration or expansion deceleration regions. Wind direction significantly impacted power output, with optimal conditions improving power coefficients by up to 33%. Škvorc and Kozmar [25] analyzed factors affecting wind energy harnessing on tall buildings. They emphasized wind resource assessment, building aerodynamics, and turbine design, favoring VAWTs for their efficiency and

lower noise in urban environments. Case studies like the Bahrain World Trade Center demonstrated potential but highlighted the need for accurate assessments and design. Significant research gaps remain, requiring further optimization for urban wind energy systems. Jooss *et al.* [26] studied the performance of a Savonius VAWT on model buildings. They found that turbine placement significantly affects power output, with the best performance at the front and center of the first building and increasing from front to back on the second. The turbine can alter available power by up to 84%, with central positions offering a good balance for urban wind energy.

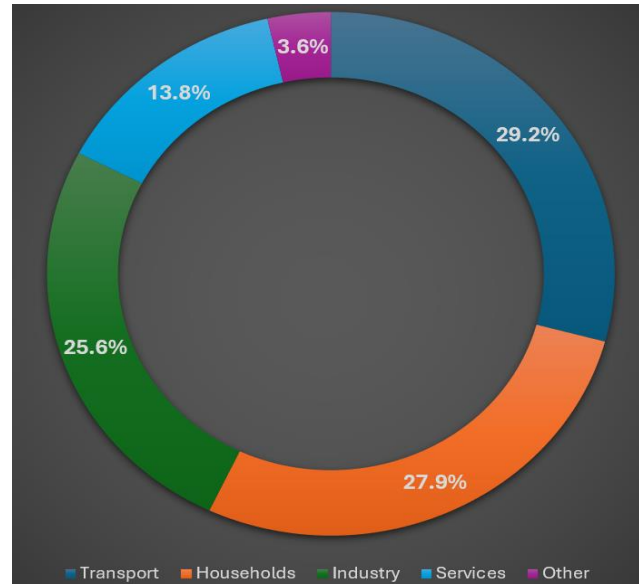


**Figure 1:** Energy consumption by sector (developed by authors).

Recent studies have explored the performance of vertical axis Ice-wind turbines. Afify [27] investigated the Ice-Wind turbine's performance, comparing it to the Savonius turbine. Conducted in a wind tunnel, the study found that a single-stage, three-blade Ice-Wind turbine with end plates, an aspect ratio of 0.38, and a blade arc angle of  $112^\circ$  performed best. The Ice-Wind turbine showed slightly higher static torque and rotational speed than the Savonius turbine, despite being more complex to manufacture, and it had a better appearance and produced less noise. Mansour and Afify [28] evaluated the Ice-Wind turbine using 3D numerical simulations with the SST K- $\omega$  model at 15.8 m/s. The Ice-Wind turbine shows slightly higher static torque (0.055 Nm) than the Savonius turbine (0.052 Nm) and generates larger, more three-dimensional vortices. Despite its manufacturing complexity, the Ice-Wind turbine has a better aesthetic and marginally improved aerodynamic performance, suggesting potential efficiency gains. Gad *et al.* [29] experimentally evaluated two, two-reversed, three, and four-blade Ice-Wind turbines. Using wind tunnel tests at 6-14 m/s, they measured static torque and rotational speed. The three-blade design showed the highest performance, with superior static torque and rotational speed, and was recommended for its efficiency and reduced noise. Turhan and Saleh [30] integrated 40 small-scale three-blade Ice-Wind turbines into a building at Istanbul Airport. Using a dynamic energy simulation tool, they achieve a 9.3% reduction in the building's annual energy consumption. The study demonstrates the significant energy-saving potential of Ice-Wind turbines when integrated into buildings.

Recent studies on Savonius wind turbines have focused on improving efficiency through blade design. This enhancement shows promise in increasing performance, making Savonius turbines a viable option for small-scale renewable energy applications. Yigit [31] optimized an S-rotor Savonius wind turbine using the RSO method. By varying aspect ratio, overlap ratio, quarter blade gap ratio, and fin configuration, the optimized S-rotor achieves a power coefficient ( $C_p$ ) of 0.104, a 65% improvement over the reference rotor's 0.063  $C_p$ . This design increases positive torque on the advancing blade and reduces negative torque on the returning blade, enhancing overall performance. Le *et al.* [32] improved a Savonius wind turbine's performance using an airfoil-shaped blade based on the FX74-CL5-140 airfoil. The new design achieves a power coefficient peak 16.5% higher than the original at a TSR of 1.1, increasing efficiency and making it suitable for urban applications. Shanegowda *et al.* [33] conducted a 3D simulation study on Savonius hydrokinetic turbines. They find that a two-blade design achieves the highest

torque coefficient of 0.295 and a power coefficient of 0.217, outperforming four-blade designs. Increasing blade numbers beyond two reduces performance due to higher drag forces. The study underscores the importance of optimizing blade design for better turbine efficiency and power output. Efendi *et al.* [34] optimized a Savonius wind turbine for residential use in Indonesia. They find a  $45^\circ$  twist angle at 5 m/s yields the best performance, achieving a  $C_p$  of 0.25 and generating 494.9 W. A grid-connected system reduces energy costs by 10.8% and CO<sub>2</sub> emissions by 53.71%. Torres *et al.* [35] improved a Savonius wind turbine using Computational Fluid Dynamics (CFD) and response surface methodology. The optimal design has an AR of 8.38, OR of 0.08, TA of  $174.05^\circ$ , and two blades, achieving a  $C_p$  of 0.21 at 12 m/s wind speed. This design provides continuous positive torque and a maximum power output of 160 W. Sonawane *et al.* [36] examined three Savonius rotor designs for low wind speeds using CFD simulations. The helical Bach rotor performs best, achieving a  $C_p$  of 0.35. Validation with a MATLAB Simulink model confirms its superior efficiency and power output for urban applications. Gemayel *et al.* [37] used LES-based CFD to study Savonius wind turbines at different Tip Speed Ratios (TSRs) and found good agreement with wind tunnel data for TSRs between 0.6 and 1.2, showing the method's effectiveness for optimizing turbine designs. This approach offers a cost-effective alternative to wind tunnel experiments. Salazar -Marín and Rodríguez-Valencia [38] designed and tested a Savonius wind turbine, validating it through simulations and wind tunnel experiments. The turbine achieves a power coefficient of 0.2, generating over 100 W at 10 m/s wind speed with a 1 m<sup>2</sup> sweep area. Redchytys *et al.* [39] studied the aerodynamic performance of Darrieus and Savonius wind turbines using CFD. The power coefficient of Darrieus rotors increases from 0.15 to 0.5, while the two-blade Savonius design achieves a higher power coefficient (0.23) than the three-blade design (0.19).

## 2. Methods

A case study was conducted on a building in Karaburun, Izmir, Türkiye, to implement wind turbine strategies. Initially, the building's energy consumption was simulated without any interventions to establish a baseline, which included both fuel and electricity usage. The study then investigated two types of Vertical Axis Wind Turbines (VAWTs): Ice-Wind Turbines and Savonius-type turbines, independently. The findings were compared to assess the effectiveness of each turbine type in reducing the building's overall energy consumption. Fig. (2) presents the flow chart of this study.

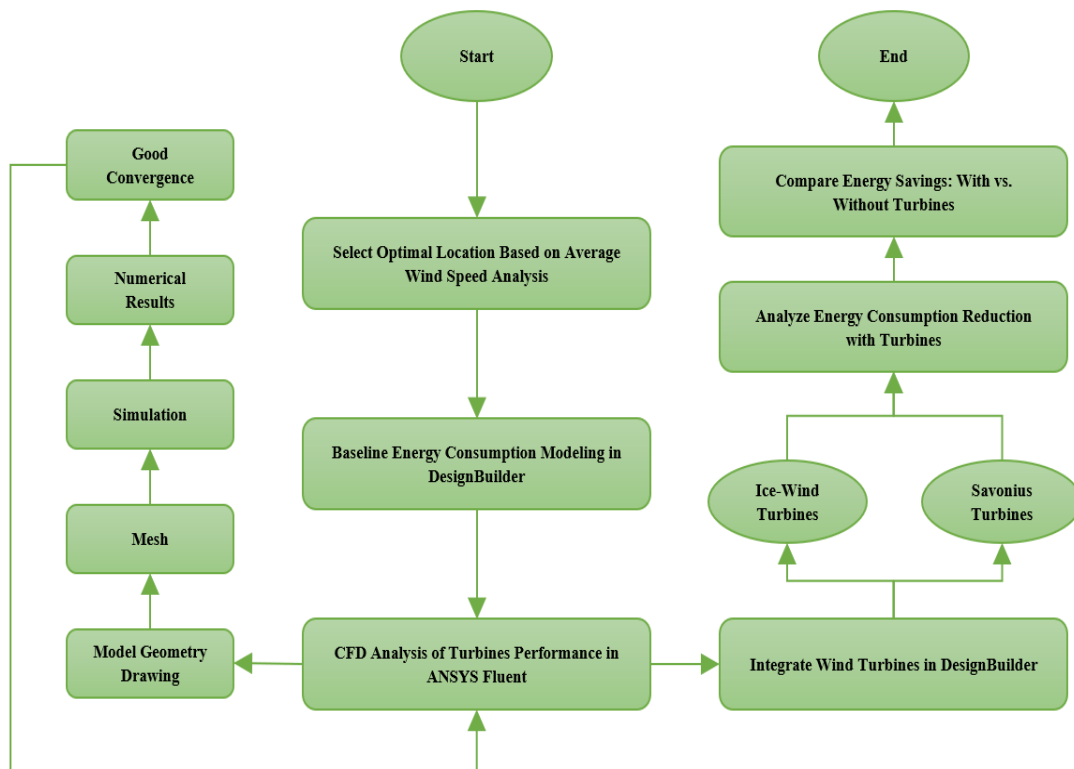


**Figure 2:** Flow chart of the study.

## 2.1. Climate and Location Analysis

Izmir, positioned in western Türkiye at coordinates (latitude 38.42° N, longitude 27.14° E), is classified under the Csa (Mediterranean) climate zone according to the Köppen-Geiger climate classification, an essential tool in climatology [40]. The Karaburun district within Izmir was selected for this study due to its optimal wind conditions. Fig. (3) shows the location of Izmir and the average wind speed in the Karaburun region [41].

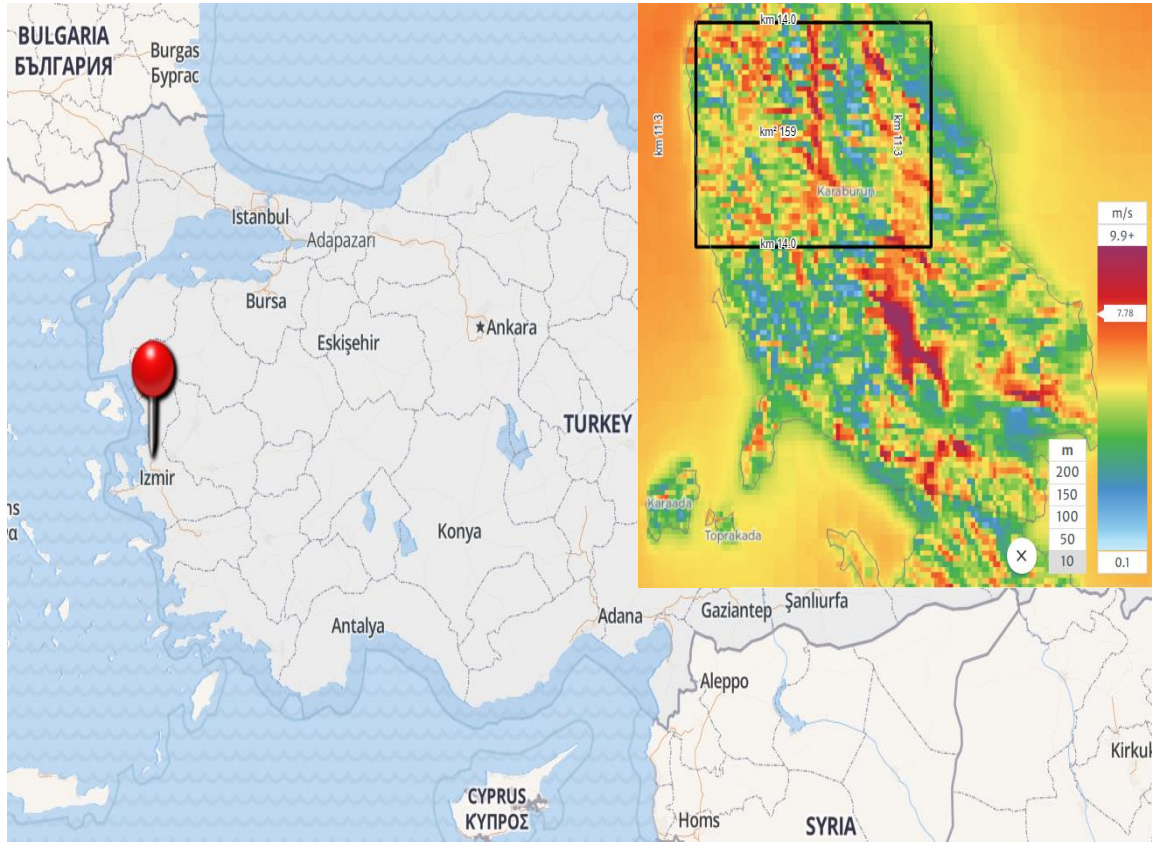


**Figure 3:** Location of Karaburun and average wind speed [41].

## 2.2 Case Building Design

The case study focuses on a residential building in the Karaburun district of Izmir, Türkiye. This two-storey structure, shown in (Fig. 4), includes a ground floor with two bedrooms, four bathrooms, a living room, a family room, a kitchen, a dining room, and storage. The first-floor features four bedrooms, four bathrooms, three dressing rooms, and a balcony. The total area of the building is 397 m<sup>2</sup>.

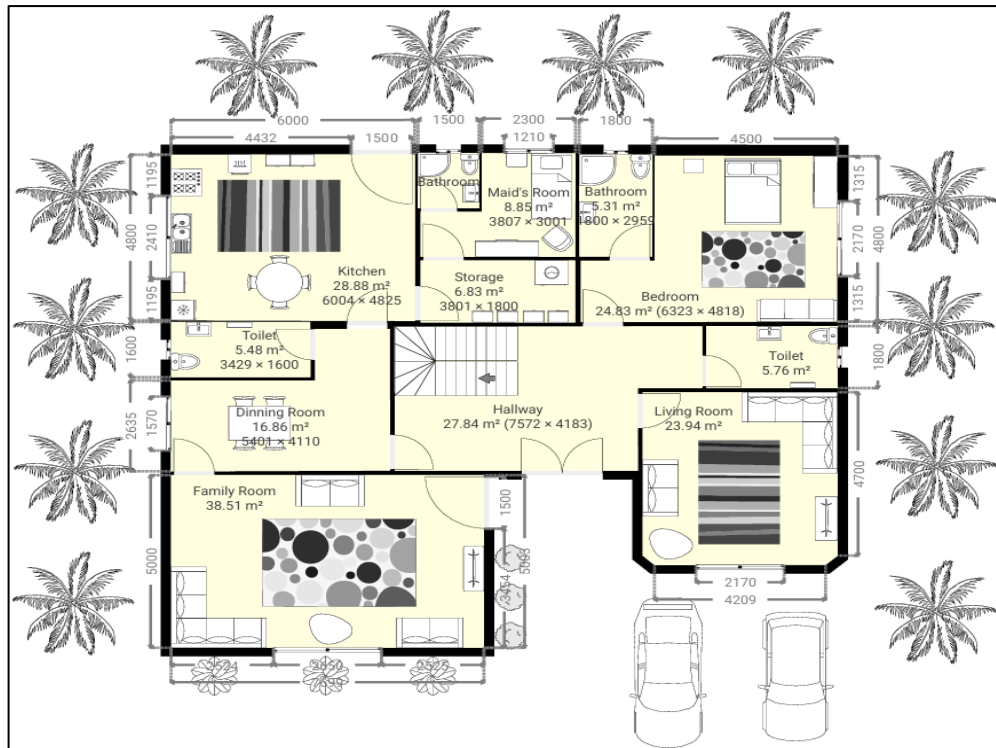
The building parameters are based on architectural drawings. Table 1 outlines the design criteria and features of the case study building. These sequential layers were referenced from [42].

The flat roof construction includes layers of gravel (0.03 m thickness, 2 W/mK thermal conductivity), bitumen felt/sheet (0.004 m thickness, 0.23 W/mK thermal conductivity), roof screed (0.03 m thickness, 0.41 W/mK thermal conductivity), foam polyurethane (0.08 m thickness, 0.028 W/mK thermal conductivity), and reinforced concrete (0.18 m thickness, 2.3 W/mK thermal conductivity). The ground floor comprises carpet/textile flooring (0.015 m thickness, 0.06 W/mK thermal conductivity), floor screed (0.05 m thickness, 0.41 W/mK thermal conductivity), reinforced concrete (0.12 m thickness, 2.3 W/mK thermal conductivity), foam polyurethane (0.07 m thickness, 0.028 W/mK thermal conductivity), and sand and gravel (0.21 m thickness, 2 W/mK thermal conductivity). The external walls are made up of cement sand render (0.015 m thickness, 1 W/mK thermal conductivity), EPS expanded polystyrene (0.08 m thickness, 0.046 W/mK thermal conductivity), medium concrete block (0.25 m



thickness, 0.51 W/mK thermal conductivity), EPS expanded polystyrene (0.03 m thickness, 0.046 W/mK thermal conductivity), and gypsum insulating plaster (0.015 m thickness, 0.18 W/mK thermal conductivity).

(a) Ground Floor



(b) First Floor

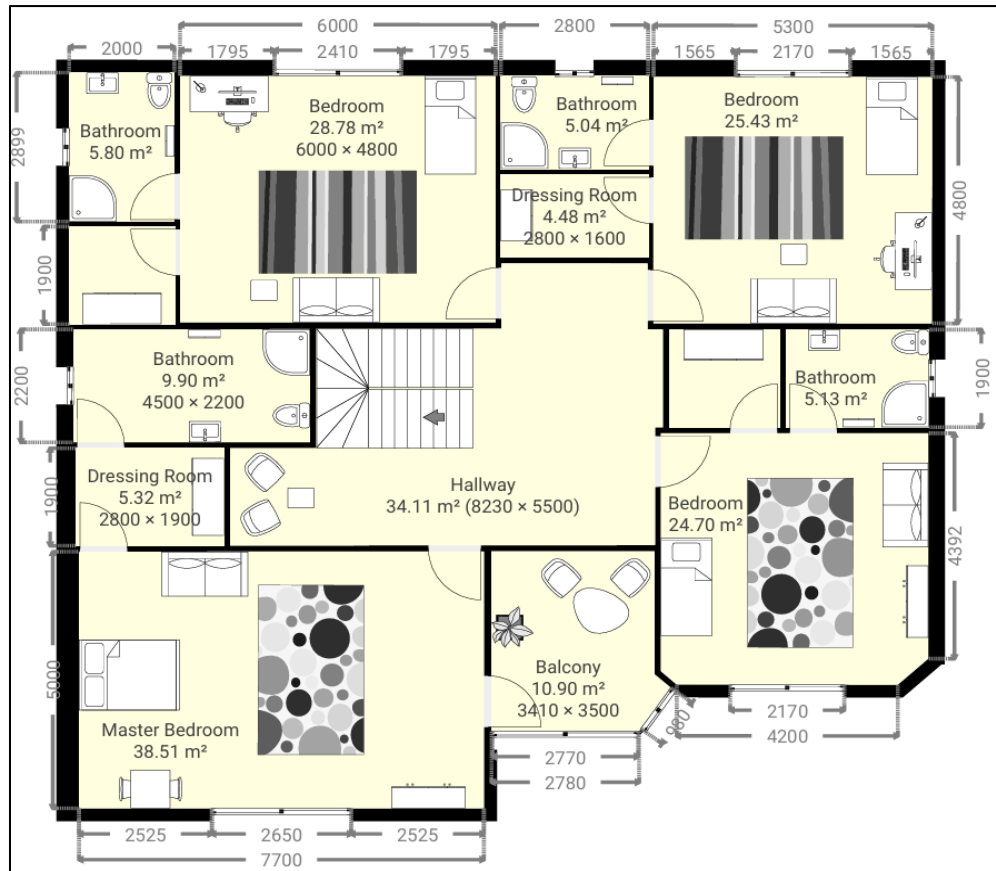


Figure 4: Architectural drawings of the Residential plan.

**Table 1: Basic design features.**

| The Building Construction Properties | Baseline Model                                    |
|--------------------------------------|---|
| Number of storeys                    | 2   |
| Overall storey area                  | 397 m <sup>2</sup>                                |
| Number of spaces                     | 26  |
| External walls (U-value)             | 0.317 (W/m <sup>2</sup> K)                        |
| Internal walls (U-value)             | 1.923 (W/m <sup>2</sup> K)                        |
| Roof (U-value)                       | 0.314 (W/m <sup>2</sup> K)                        |
| Ground floor (U-value)               | 0.309 (W/m <sup>2</sup> K)                        |
| Glazing type + U-value               | Reference glazing with 1.978 (W/m <sup>2</sup> K) |

### 2.3. Energy Simulation Analysis

An hourly dynamic building simulation tool, DesignBuilder, was utilized to simulate the baseline model and various energy-efficient design strategies [43]. The materials for the case building were sourced from architectural drawings, and the construction model adheres to the values specified in Table 1. Fig. (5) shows the three-dimensional baseline model. To ensure accurate results, the building simulated weather data from IZMIR-TUR IWEC was used. The simulation considers three scenarios: The first one without any solutions, and the other solutions are small-scale Ice-Wind and Savonius turbines.

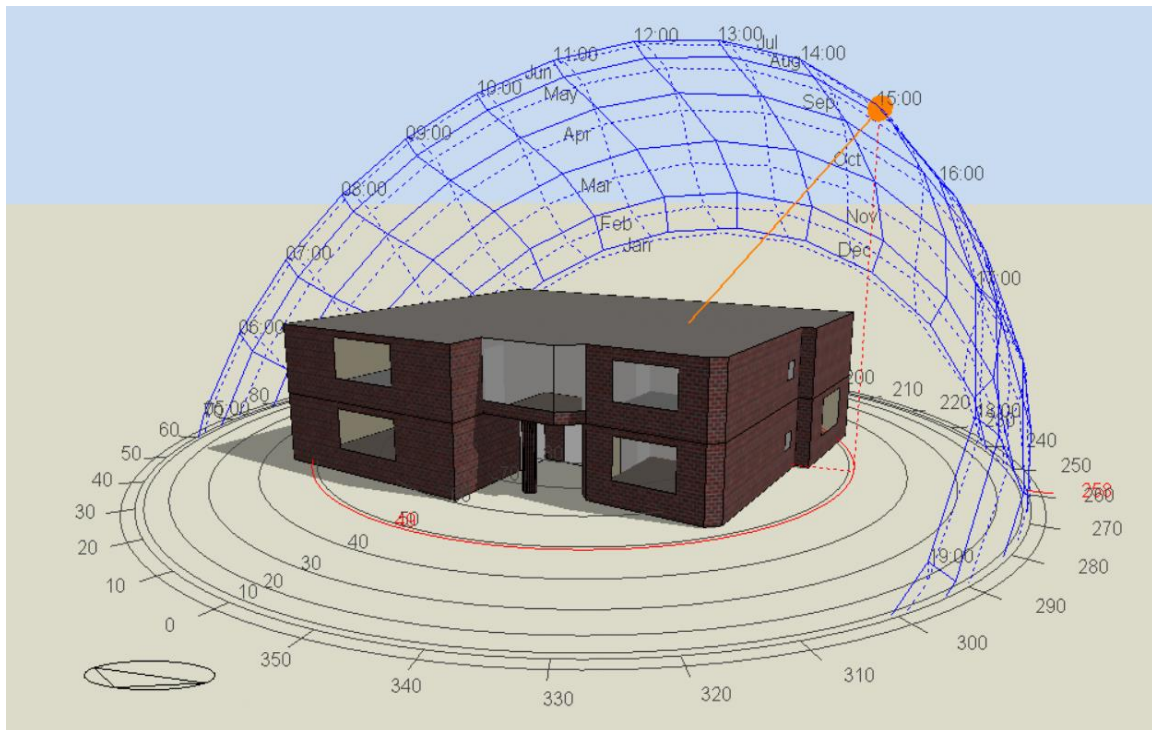


**Figure 5:** Energy Simulation Model of the Case Building.

### 2.4. Retrofitting Strategies

Two energy-efficient design strategies were applied to the case building. The objective of these strategies was to evaluate their impact on lowering energy consumption in residential buildings and reducing environmental pollution by utilizing sustainable energy sources.

### 2.4.1. Case One: Building-Integrated Ice-Wind Turbine

A small-scale Ice-Wind turbine was designed for the case building, featuring fifteen turbines mounted on the roof. These turbines were carefully arranged to make optimal use of the rooftop space and maximize wind energy capture, with appropriate spacing to prevent aerodynamic interference. The turbine blades were designed by Saleh *et al.* [44] using SolidWorks software [45], resulting in each turbine having a diameter of 0.757 [44] and a height of 1.456 m, and a swept area of 1.95 m<sup>2</sup>, as calculated by the software. Fig. (6) illustrate the design of the Ice-Wind turbine. Fig. (7) shows the design of the three-blade Ice-Wind Vertical Axis Wind Turbine (VAWT) mounted on the case building.

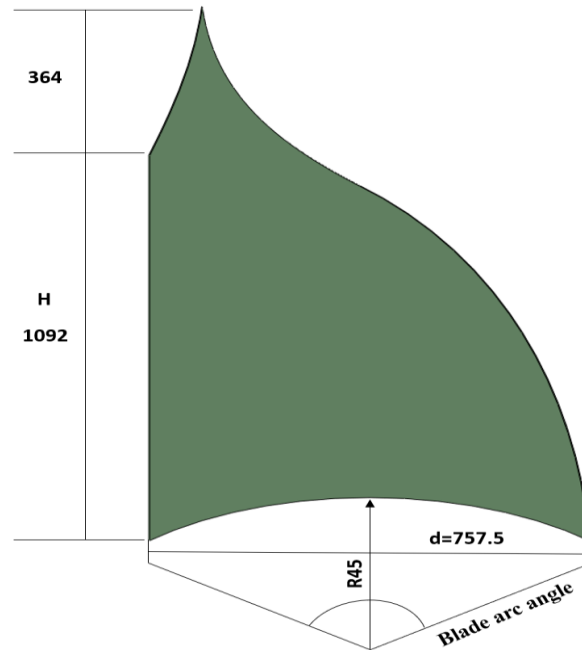


**Figure 6:** Ice-Wind turbine dimensions.

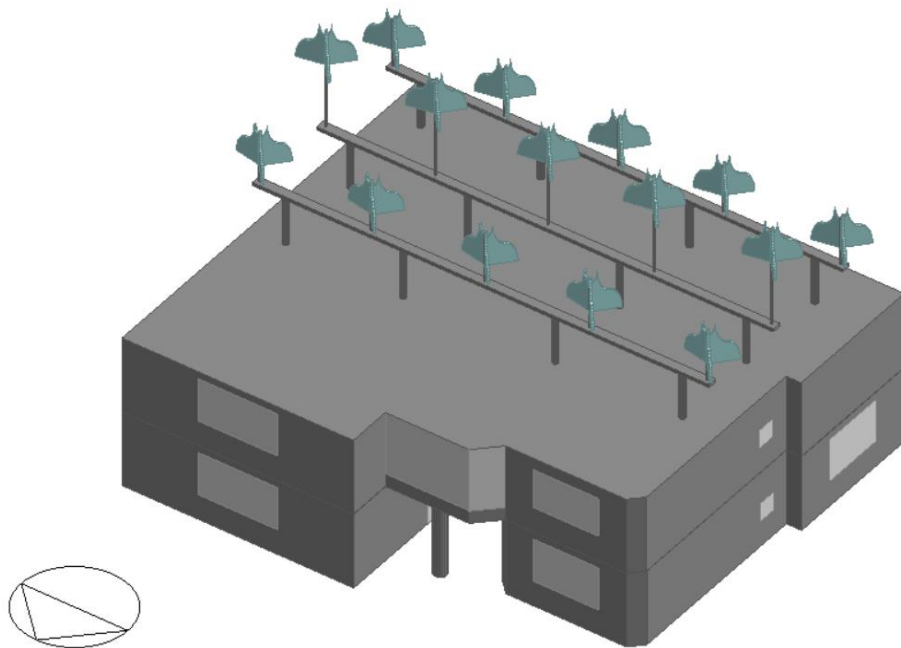


**Figure 7:** Ice-Wind turbines mounted on the building (developed by authors).



**2.4.2. Case Two: Building-Integrated Savonius Wind Turbine**

A small-scale Savonius turbine setup was developed specifically for the case building, incorporating fifteen turbines installed on the roof. The blades for these turbines were crafted using SolidWorks software, giving each turbine a diameter of 1.515 m, a height of 1.456 m, and a swept area of 2.28 m<sup>2</sup>, as determined by the software. Fig. (8) illustrates the design of the two-blade Savonius type. Fig. (9) depicts three concrete beams on top of the case building, supported by columns proportional to the size of the structures. Each concrete column houses five Savonius wind turbines. These turbines were strategically distributed across the building to reduce energy consumption in the case study building.

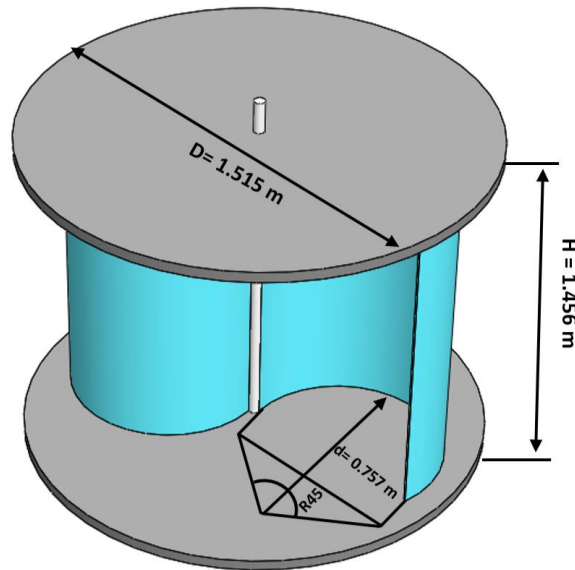


**Figure 8:** Savonius Wind Turbine Dimensions.

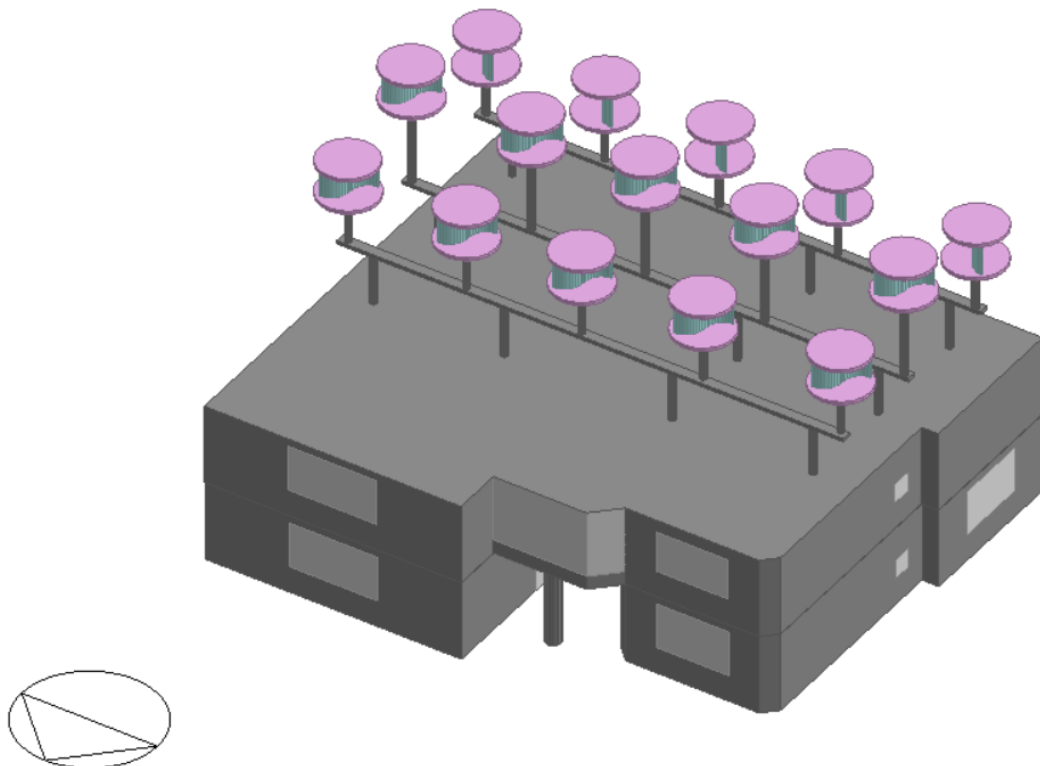


**Figure 9:** Savonius turbines mounted on the building (developed by authors).

Airflow simulations around the Savonius turbine were carried out using a 3D domain with dimensions of 9m × 5m × 4m in ANSYS Fluent Software [46]. The model includes a velocity inlet boundary where wind enters at 11.67 m/s, a pressure outlet for air exit, and no-slip boundary conditions on all remaining surfaces.

The simulation employed a tetrahedral mesh with 927,629 nodes and 5,053,136 elements, chosen to enhance result accuracy. The study utilized the Shear Stress Transport (SST) K- $\omega$  model, known for its precision in predicting the aerodynamic performance of VAWTs [47, 48]. Fig. (10) presents the boundary conditions and the mesh of the Savonius wind turbine domain from a side view.

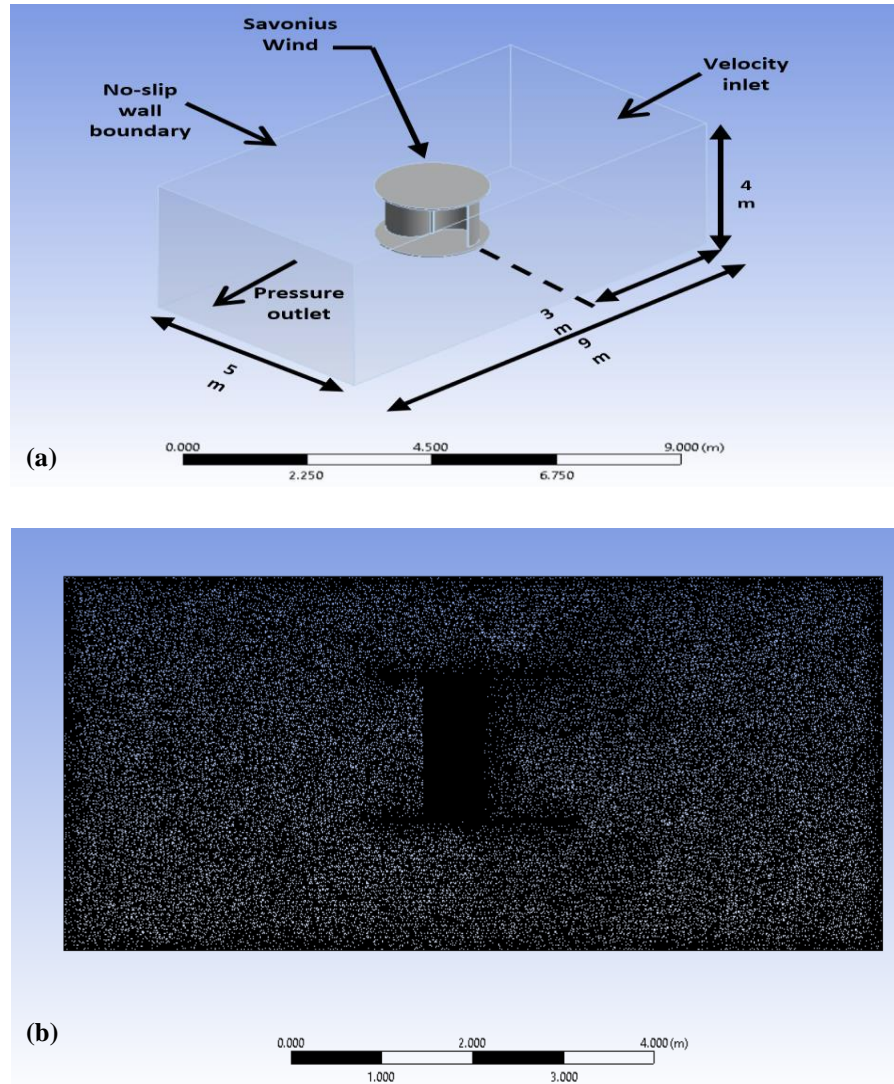


**Figure 10:** Savonius model in Ansys: (a) The Savonius turbine and domain dimensions (m); (b) Mesh of the Savonius turbine domain from side view.

The average wind speed for the Karaburun location is recorded at 7.78 m/s. Simulation results indicate that the rated power output reaches 502 W, with the rotor operating at a speed of 200 rev/min and a tip speed ratio of 1.38. Table 2 details the input parameters for the building-integrated wind turbines.

The transport equations are used to calculate the turbulent kinetic energy equations (2.1) and (2.2):

$$\frac{\partial}{\partial t}(\rho k) + \frac{\partial}{\partial x_i}(\rho k u_i) = \frac{\partial}{\partial x_j} \left( \Gamma_k \frac{\partial k}{\partial x_j} \right) + G_k + Y_k + S_k + G_b \quad (2.1)$$

$$\frac{\partial}{\partial t}(\rho\omega) + \frac{\partial}{\partial x_i}(\rho\omega u_i) = \frac{\partial}{\partial x_j}\left(\Gamma_\omega \frac{\partial \omega}{\partial x_j}\right) + G_\omega + Y_\omega + S_\omega + G_{\omega b} \quad (2.2)$$

**Table 2: Input parameters of wind turbine.**

| Input Parameter        |       | Input Parameter                       |                            |
|------------------------|-------|---------------------------------------|----------------------------|
| Operation type         | 24/7  | Cut out wind speed (m/s)              | 3.5                        |
| Rotor speed (rev/min)  | 200   | Cut in wind speed (m/s)               | 25                         |
| Rotor diameter (m)     | 1.515 | Maximum tip speed ratio               | 1.38                       |
| Number of blades       | 2     | Maximum power coefficient             | 0.23                       |
| Rated power output (W) | 502   | Annual local average wind speed (m/s) | 7.78                       |
| Rated wind speed (m/s) | 10    | Power control                         | Fixed speed variable pitch |

In these two equations,  $G_k$  is the turbulence kinetic energy due to mean velocity gradients.  $G_\omega$  denotes the generation of  $\omega$ .  $\Gamma_k$  and  $\Gamma_\omega$  refer the effective diffusivity of  $k$  and  $\omega$ , correspondingly.  $Y_k$  and  $Y_\omega$  symbolize the dissipation of  $k$  and  $\omega$ , respectively, due to turbulence.  $G_k$  and  $G_{\omega b}$  account for buoyancy terms.  $S_k$  and  $S_\omega$  are defined by the user as source terms [49].

Obtaining rated wind speed [50] from equation (2.6). The power coefficient, torque coefficient, and tip speed ratio are obtained from the following equations correspondingly:

$$C_P = \frac{P_{Turbine}}{P_{available}} = \frac{P_{Turbine}}{0.5\rho A_s V^3} \quad (2.3)$$

$$C_T = \frac{T}{0.5\rho A_s V^2 R} \quad (2.4)$$

$$\lambda = \frac{R \cdot \omega}{V} \quad (2.5)$$

$$V_{rated} = 1.5V_{average} \quad (2.6)$$

$P_{Turbine}$ : Power output (watts)

$\rho$ : Air density (kg/m<sup>3</sup>)

$A_s$ : Swept area (m<sup>2</sup>)

$V$ : Wind speed (m/s)

$T$ : Torque (N.m)

$\lambda$ : Tip speed ratio

$R$ : Radius of the rotor (m)

$\omega$ : Rotational speed (rad/s)

$V_{rated}$ : Rated wind speed (m/s)

$P_{Turbine}$  refers to the turbine's power output in watts, while  $A_s$  denotes the swept area of the rotor in square meters (m<sup>2</sup>).  $\rho$  (rho) is the air density in kg/m<sup>3</sup>, and  $V$  represents wind speed in meters per second (m/s).  $T$  indicates torque in newton-meters (Nm),  $R$  is the rotor radius in meters (m), and  $\omega$  (omega) signifies the angular velocity in radians per second (rad/s).

The Ice-Wind turbine was analyzed using a similar CFD approach as the Savonius turbine. The simulation involved setting up a 3D domain with appropriate boundary conditions, including a velocity inlet, pressure outlet,

and no-slip conditions on solid surfaces. A tetrahedral mesh was utilized to ensure accurate resolution of flow features, and the SST  $k-\omega$  turbulence model was employed for its reliability in predicting aerodynamic performance. The analysis focused on the distribution of pressure and velocity around the turbine blades, with results indicating the flow patterns and potential areas for optimization.

To assess the economic feasibility of the small-scale wind turbine, determining the payback period. This crucial financial metric indicates the time needed to recover the investment in the wind turbine through its energy savings or generated revenue. The payback period is computed using the following equation:

$$\text{Payback Period} = \frac{\text{Total Initial Investement}}{\text{Annual Net Savings or Revenue}} \quad (2.7)$$

### 3. Results and Discussion

Used dynamic and velocity pressures to understand flow dynamics and their impact on turbine performance. Our focus was on assessing aerodynamic efficiency and energy capture potential, rather than detailed blade design, aligning with our study's emphasis on the practical application of Ice-Wind and Savonius turbines in urban residential settings.

The dynamic pressure distribution indicates a peak value of 226.0 Pa and a minimum of 3.49e-06 Pa, with high-pressure zones on the wind-facing edges of the blades and low-pressure areas in the wake behind the blades. The velocity magnitude distribution shows a maximum of 19.1 m/s and a minimum of 1.91e-06 m/s Fig. (11), with high velocities at the blade tips and gaps, essential for energy capture, and low velocities behind the blades signifying turbulence.

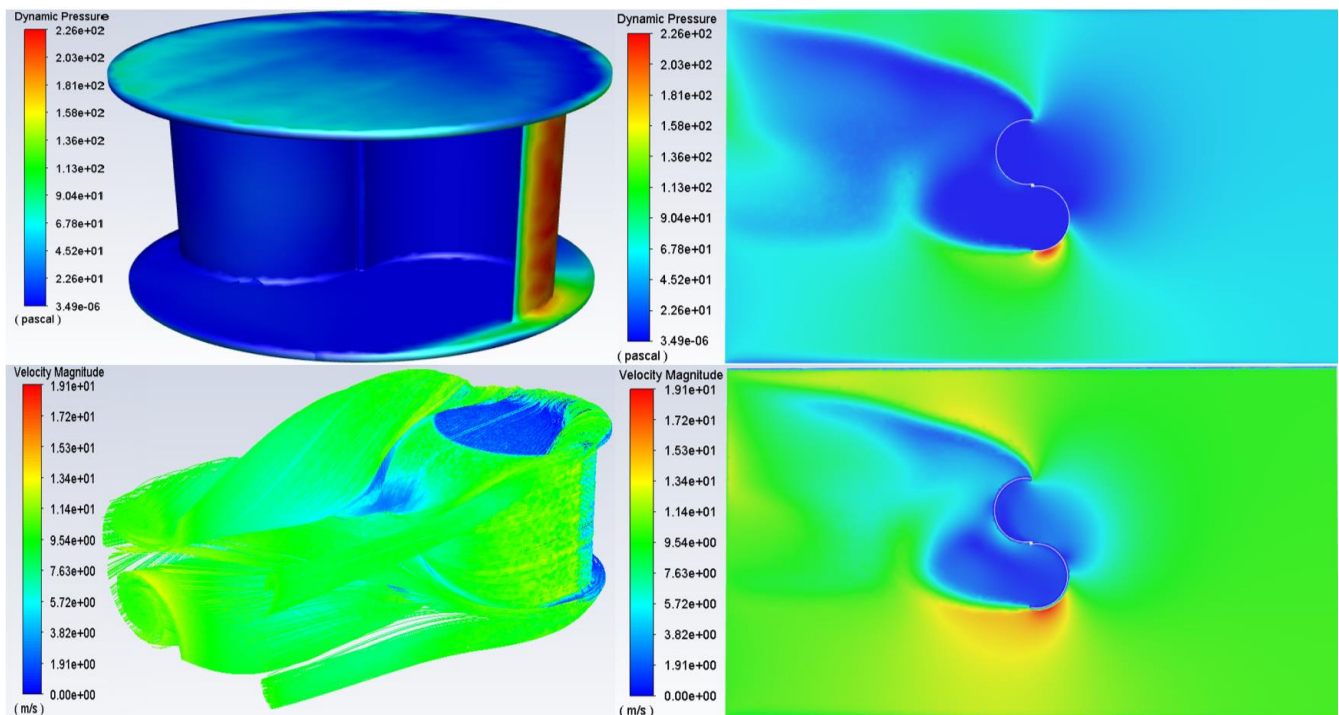


**Figure 11:** Pressure distributions and velocity magnitude of Savonius turbine: (a) Dynamic pressure; (b) velocity magnitude.

The analysis focuses on the distribution of dynamic pressure and velocity magnitude, as well as flow streamlines around the turbine blades under a wind speed of 10 m/s. Fig. (12a) presents the turbine in both 3D and 2D views, displaying dynamic pressure values ranging from 0.00107 Pa to 254 Pa. Fig. (12b) shows the airflow velocity magnitude in 3D and 2D, with a peak speed of 19.8 m/s.

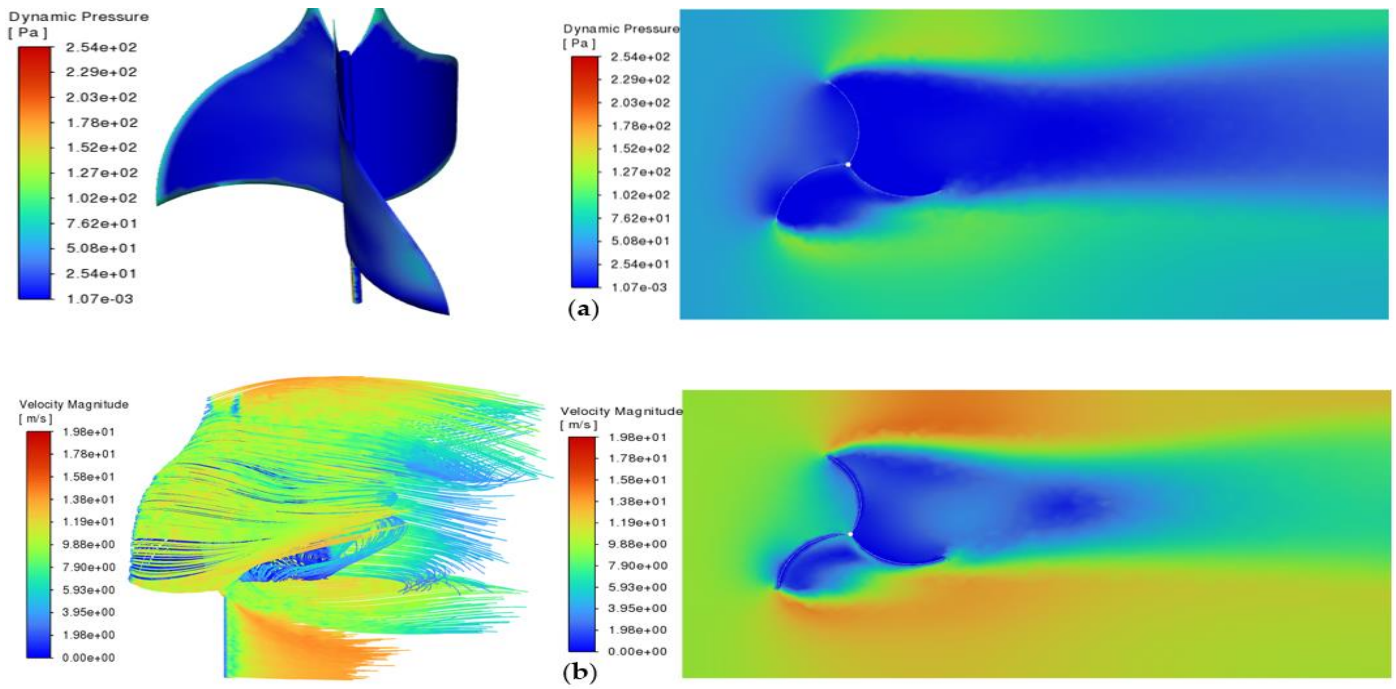


**Figure 12:** Pressure distributions and velocity magnitude of Ice-wind turbine: (a) Dynamic pressure; (b) velocity magnitude [44].

Upon integrating all previously discussed cases in Section (2), the results for each scenario are detailed in the Table 3 below:

**Table 3: Simulation results for all cases.**

| Model Name     | Energy Consumption (KWh/m <sup>2</sup> ) | Energy Saving % | Payback Period (Years) |
|----------------|--|-----------------|------------------------|
| Baseline model | 155.7                                    | -               | -                      |
| Case 1         | 120                                      | 22.5            | 14.57                  |
| Case 2         | 99.6                                     | 36              | 8.93                   |

The economic assessment of the turbines incorporated an initial investment of \$2,000 and an annual maintenance cost of \$50. The Savonius turbine, with a rated power output of 502 watts, was estimated to generate 4395.12 kWh annually, while the Ice-Wind turbine, with a rated power of 305 watts, was projected to produce 2674.8 kWh annually. Considering the local electricity price of \$0.07 per kWh, the payback periods were calculated, showing that the Savonius turbine could achieve a payback period of 8.93 years with a 36% energy saving, while the Ice-Wind turbine had a longer payback period of 14.57 years with a 22.5% energy saving.

The materials and thermal conductivity parameters used in the simulation are crucial for accurately modeling the energy consumption of the building. The chosen materials reflect common construction practices in Izmir, Turkey, and are aligned with the local standards, such as those specified by the Turkish Standards Institution (TS 825). These parameters significantly impact the building's thermal performance and energy consumption, thereby providing a realistic baseline for the analysis of energy savings achieved through the integration of wind turbines.

The integration of these wind turbines into residential buildings resulted in significant energy savings. The baseline model, with an energy consumption of 155.7 kWh/m<sup>2</sup>, was reduced to 120 kWh/m<sup>2</sup> with the implementation of Ice-Wind turbines, achieving a 22.5% reduction. In contrast, the use of Savonius turbines brought the energy consumption down to 99.6 kWh/m<sup>2</sup>, resulting in a 36% reduction. These results show the effectiveness of Savonius turbines in reducing overall energy consumption and highlight their potential for broader application in residential buildings to enhance sustainability and reduce environmental impact.



The payback period calculation for both the Ice-Wind and Savonius turbines includes a detailed cost analysis of purchase expenses, installation, and maintenance. The initial purchase cost for each Ice-Wind turbine is approximately \$2000, while each Savonius turbine costs about \$2300. Installation costs are estimated at \$500 per turbine, which covers labor and necessary equipment. Additionally, an annual maintenance fee of \$50 per turbine is factored into the analysis to account for routine checks and minor repairs. While the current analysis does not include any subsidies or incentives, it is worth noting that potential government grants or tax incentives for renewable energy installations could significantly reduce the payback period. Moreover, long-term maintenance and potential degradation of the turbines could affect actual pay-back period.

In discussing the findings, it is important to acknowledge certain limitations. The results are based on simulations specific to Izmir's wind conditions and a single building type, which may limit their generalizability to other regions and building configurations. Additionally, assumptions made during the simulations, such as the use of idealized wind conditions and building models, could influence the outcomes. These factors should be considered when applying the findings to different contexts, and further research is needed to explore the scalability and adaptability of these solutions in diverse environments.

## 4. Conclusion

This study has demonstrated the significant potential of integrating small-scale vertical axis wind turbines (VAWTs) into residential buildings to reduce energy consumption and promote sustainability. By focusing on two types of VAWTs, the Ice-Wind and Savonius turbines, we were able to compare their efficacy and economic feasibility. The Savonius turbine emerged as the more efficient option, providing a 36% reduction in energy consumption with a relatively short payback period of 8.93 years, compared to the Ice-Wind turbine's 22.5% reduction and 14.57-year payback period.

Dynamic pressure and velocity distribution analyses underscored the importance of blade design and placement in optimizing turbine performance. High-pressure zones on the windward side and high velocities at the blade tips were critical for maximizing energy capture. The study's economic evaluation, considering initial investment and maintenance costs, further validated the practicality of these renewable energy solutions.

The findings from this research highlight the tangible benefits of integrating VAWTs into residential infrastructure, particularly in regions with favorable wind conditions like Karaburun, Izmir. By reducing reliance on fossil fuels and lowering overall energy consumption, these turbines contribute to the global efforts toward achieving near-zero energy buildings. Future research should continue to explore optimization strategies for turbine design and placement, as well as investigate the long-term performance and durability of these systems in various climatic conditions.

In conclusion, the adoption of Savonius and Ice-Wind turbines represents a viable and effective approach to enhancing energy efficiency in residential buildings, paving the way for more sustainable and environmentally friendly urban development.

## Conflict of Interest

The authors declare that there are no conflicts of interest regarding the publication of this paper.

## Funding Information

The authors declare that this research received no specific grant from any funding agency in the public, commercial, or not-for-profit sectors.

## References

- [1] International Energy Agency (IEA). World Energy Outlook 2023. Paris: IEA; 2023. Available from: <https://www.iea.org/reports/world-energy-outlook-2023> (accessed on June 2024).

- [2] International Energy Agency. Electricity Market Report 2023. International Energy Agency, 2023. Available from: <https://www.iea.org/reports/electricity-market-report-2023>
- [3] Turhan C, Ghazi S. Energy consumption and thermal comfort investigation and retrofitting strategies for an educational building: case study in a temperate climate zone. *J Build Des Environ*. 2023; 2(2): 16869. <https://doi.org/10.37155/2811-0730-0201-7>
- [4] Saygin D, Hoffman M, Godron P. How Turkey can ensure a successful energy transition. Center for American Progress, 2018. Available from: <https://www.americanprogress.org/issues/green/reports/2018/07/16/451580/turkey-can-ensure-successful-energy-transition/>
- [5] Smart Güneş Enerjisi Teknolojileri Ar-Ge Üretim Sanayi ve Ticaret A.Ş. 01.01.2023 – 30.06.2023 Dönemine Ait Faaliyet Raporu. Available from: <https://www.smartsolar.com.tr/>
- [6] PwC. Dünyada ve Türkiye'de Güneş Enerjisi Sektörü. PwC, Mart 2024. Available from: <http://www.pwc.com.tr/>
- [7] IRENA. World Energy Transitions Outlook 2023: 1.5°C Pathway. International Renewable Energy Agency, 2023. Available from: <https://www.irena.org/publications>
- [8] Hafez FS, Sa'di B, Safa-Gamal M, Taufiq-Yap YH, Alrifayy M, Seyedmahmoudian M, *et al.* Energy efficiency in sustainable buildings: a systematic review with taxonomy, challenges, motivations, methodological aspects, recommendations, and pathways for future research. *Energy Strat Rev*. 2023; 45: 101013. <https://doi.org/10.1016/j.esr.2022.101013>
- [9] Camarasa C, Kalahasthi LK, Rosado L. Drivers and barriers to energy-efficient technologies (EETs) in EU residential buildings. *Energy and Built Environment*, 2021; 2: 290-301. <https://doi.org/10.1016/j.enbenv.2020.08.002>
- [10] Razmjoo A, Mirjalili S, Aliehyaei M, Østergaard PA, Ahmadi A, Nezhad MM. Development of smart energy systems for communities: technologies, policies, and applications. *Energy*. 2022; 248: 123540. <https://doi.org/10.1016/j.energy.2022.123540>
- [11] Li Y, Kubicki S, Guerriero A, Rezgui Y. Review of building energy performance certification schemes towards future improvement. *Renew Sustain Energy Rev*. 2019; 113: 109244. <https://doi.org/10.1016/j.rser.2019.109244>
- [12] Chen L, Hu Y, Wang R, Li X, Chen Z, Hua J, *et al.* Green building practices to integrate renewable energy in the construction sector: a review. *Environ Chem Lett*. 2024; 22: 751-84. <https://doi.org/10.1007/s10311-023-01675-2>
- [13] Di Foggia G. Energy efficiency measures in buildings for achieving sustainable development goals. *Heliyon*, 2018; 4. <https://doi.org/10.1016/j.heliyon.2018.e00953>.
- [14] Li J, Shui B. A comprehensive analysis of building energy efficiency policies in China: status quo and development perspective. *J Cleaner Prod*. 2015; 90: 326-44. <https://doi.org/10.1016/j.jclepro.2014.11.061>
- [15] Yeatts DE, Auden D, Cooksey C, Chen CF. A systematic review of strategies for overcoming the barriers to energy-efficient technologies in buildings. *Energy Res Social Sci*. 2017; 32: 76-85. <https://doi.org/10.1016/j.erss.2017.03.010>
- [16] Labanca N, Suerkemper F, Bertoldi P, Irrek W, Duplessis B. Energy efficiency services for residential buildings: market situation and existing potentials in the European Union. *J Cleaner Prod*. 2015; 109: 284-95. <https://doi.org/10.1016/j.jclepro.2015.02.077>
- [17] Bertoldi P, Economidou M, Palermo V, Boza-Kiss B, Irrek W, Duplessis B. How to finance energy renovation of residential buildings: Review of current and emerging financing instruments in the EU. *WIREs Energy Environ*. 2020; 10. <https://doi.org/10.1002/wene.384>
- [18] Shen L, He B, Jiao L, Song X, Zhang X. Research on the development of main policy instruments for improving building energy-efficiency. *J Cleaner Prod*. 2016; 112: 1789-1803. <https://doi.org/10.1016/j.jclepro.2015.06.108>
- [19] Giraudet LG. Energy efficiency as a credence good: A review of informational barriers to energy savings in the building sector. *Energy Econ*. 2020; 87:104698. <https://doi.org/10.1016/j.eneco.2020.104698>
- [20] Kyriakopoulos GL, Arabatzis G. Electrical energy storage systems in electricity generation: Energy policies, innovative technologies, and regulatory regimes. *Renew Sustain Energy Rev*. 2016; 56: 1044-67. <https://doi.org/10.1016/j.rser.2015.12.046>
- [21] Basher MK, Nur-E-Alam M, Rahman MM, Alameh K, Hinckley S. Aesthetically appealing building integrated photovoltaic systems for net-zero energy buildings: current status, challenges, and future developments—a review. *Buildings*. 2023; 13: 863. <https://doi.org/10.3390/buildings13040863>
- [22] Wilberforce T, Olabi AG, Sayed ET, Elsaid K, Maghrabie HM, Abdelkareem MA. A review on zero energy buildings – Pros and cons. *Energy Built Environ*. 2023; 4: 25-38. <https://doi.org/10.1016/j.enbenv.2021.06.002>
- [23] Calautit K, Johnstone C. State-of-the-art review of micro to small-scale wind energy harvesting technologies for building integration. *Energy Convers Manag*. 2023; 20:100457. <https://doi.org/10.1016/j.ecmx.2023.100457>
- [24] Xu W, Li Y, Li G, Li S, Zhang C, Wang F, *et al.* High-resolution numerical simulation of the performance of vertical axis wind turbines in urban area: Part II, array of vertical axis wind turbines between buildings. *Renew Energy*. 2021; 176:25-39. <https://doi.org/10.1016/j.renene.2021.05.011>
- [25] Škvorc P, Kozmar H. Wind energy harnessing on tall buildings in urban environments. *Renew Sustain Energy Rev*. 2021; 152: 111662. <https://doi.org/10.1016/j.rser.2021.111662>
- [26] Jooss Y, Bolis R, Bracchi T, Hearst RJ. Flow field and performance of a vertical-axis wind turbine on model buildings. *Flow*. 2022; 2. <https://doi.org/10.1017/flo.2022.3>
- [27] Afify R. Experimental studies of an icewind turbine. *Int J Appl Eng Res*. 2019; 14(17): 3633-45.
- [28] Mansour H, Afify R. Design and 3D CFD static performance study of a two-blade icewind turbine. *Energies*. 2020; 13(20): 5356. <https://doi.org/10.3390/en13205356>

- [29] Gad T, Shokry A, Afify R, Saber E, Hasan M. Experimental study of two, two-reversed, three and four blade icewind turbine. *Int J Appl Eng Res.* 2020; 15(12): 1122-34.
- [30] Turhan C, Saleh YAS. A case study for small-scale vertical wind turbine integrated building energy saving potential. *J Build Des Environ.* 2024; 3(1): 28115. <https://doi.org/10.37155/2811-0730-0301-5>
- [31] Yigit C. Numerical investigation of specific performance parameters of the S-ROTOR; a Savonius type turbine design. *Ocean Eng.* 2024; 291: 116314. <https://doi.org/10.1016/j.oceaneng.2023.116314>
- [32] Le AD, Thu PNT, Doan VH, Tran HT, Banh MD, Troung V. Enhancement of aerodynamic performance of Savonius wind turbine with airfoil-shaped blade for the urban application. *Energy Conversion and Management*, 2024; 310: 118469. <https://doi.org/10.1016/j.enconman.2024.118469>
- [33] Shanegowda TG, Shashikumar CM, Gumptapure V, Madav V. Numerical studies on the performance of Savonius hydrokinetic turbines with varying blade configurations for hydropower utilization. *Energy Convers Manag.* 2024; 312: 118535. <https://doi.org/10.1016/j.enconman.2024.118535>
- [34] Efendi MY, Amir N, Prasetyo T, Ramadhan MY, Gozan M, Darmawan MA. Experimental and simulation investigation of a Savonius vertical axis wind turbine for residential applications: a case study in Indonesia. *Int J Ambient Energy.* 2024; 45(1): 2331241. <https://doi.org/10.1080/01430750.2024.2331241>
- [35] Torres S, Marulanda A, Montoya MF, Hernandez C. Geometric design optimization of a Savonius wind turbine. *Energy Convers Manag.* 2022; 262: 115679. <https://doi.org/10.1016/j.enconman.2022.115679>
- [36] Sonawane CR, Sasar Y, Shaikh M, Kokande Y, Mustafa M, Pandey A. Numerical simulation of Savonius rotors used for low wind speed application. *Materials Today: Proceedings.* 2022; 49: 1610-1616. <https://doi.org/10.1016/j.matpr.2021.07.420>
- [37] Gemayel D, Abdelwahab M, Ghazal T, Aboshosha H. Modelling of vertical axis wind turbine using large eddy simulations. *Results Eng.* 2023; 18: 101226. <https://doi.org/10.1016/j.rineng.2023.101226>
- [38] Salazar-Marín EA, Rodriguez-Valencia AF. Design, assembly and experimental tests of a Savonius type wind turbine. *Scientia et Technica*, 2019; 24(3): 397-407. <https://doi.org/10.22517/23447214.20411>
- [39] Redchytys D, Portal-Porras K, Tarasov S, Moiseienko S, Tuchyna U, Starun N. Aerodynamic performance of vertical-axis wind turbines. *J Marine Sci Eng.* 2023; 11: 1367. <https://doi.org/10.3390/jmse11071367>
- [40] Kottek M, Grieser J, Beck C, Rudolf B, Rubel F. World Map of the Köppen-Geiger climate classification updated. *Meteorologische Zeitschrift*, 2006; 15(3): 259-63. <https://doi.org/10.1127/0941-2948/2006/0130>
- [41] Global Wind Atlas. Available online: <https://globalwindatlas.info/ar> (accessed on May 2024).
- [42] Türk Standardları Enstitüsü. TS 825: Thermal Insulation Requirements for Buildings. Türk Standardları Enstitüsü, Ankara, 2008. Available online: <https://intweb.tse.org.tr> (accessed on May 2024).
- [43] DesignBuilder, v.6.1.0.006. Available from: <http://www.designbuilder.co.uk/> (accessed on May 2024).
- [44] Saleh YAS, Akkurt GG, Turhan C. Reconstructing Energy-Efficient Buildings after a Major Earthquake in Hatay, Türkiye. *Buildings*, 2024; 14:2043. Available from: <https://doi.org/10.3390/buildings14072043>
- [45] Solidworks, 2018. Available from: <https://www.solidworks.com/> (accessed on May 2024).
- [46] ANSYS, Inc. ANSYS Fluent, 2020. Available online: <https://www.ansys.com/> (accessed on May 2024).
- [47] Eltayesh A, Castellani F, Natili F, Burlando M, Khedr M. Aerodynamic upgrades of a Darrieus vertical axis small wind turbine. *Energy Sustain Dev.* 2023; 73: 126-43. <https://doi.org/10.1016/j.esd.2023.01.018>
- [48] Zidane IF, Ali HM, Swadener G, Eldrainy YA, Shehata AI. Effect of upstream deflector utilization on H-Darrieus wind turbine performance: An optimization study. *Alexandria Eng J.* 2023; 63:175-89. <https://doi.org/10.1016/j.aej.2022.07.052>
- [49] Fertahi S, Samaouali A, Kadiri I. CFD comparison of 2D and 3D aerodynamics in H-Darrieus prototype wake. *e-Prime - Adv Electric Eng Electron Energy.* 2023; 4: 100178. <https://doi.org/10.1016/j.prime.2023.100178>
- [50] Venkata Sai SJ, Venkateswara Rao T. Design and analysis of vertical axis savonius wind turbine. *Int J Eng Technol.* 2016; 8(2): 1069-76. <https://doi.org/10.1111/ijet.2016.08.02>